Performance comparison of small-pixel CdZnTe radiation detectors with gold contacts formed by sputter and electroless deposition

Published by IOP Publishing for Sissa Medialab

Received: *March 3, 2017*
Revised: *May 21, 2017*
Accepted: *June 1, 2017*
Published: *June 26, 2017*

Performance comparison of small-pixel CdZnTe radiation detectors with gold contacts formed by sputter and electroless deposition

S.J. Bell,[a,b,c,1,2] **M.A. Baker,**[b] **D.D. Duarte,**[a,b] **A. Schneider,**[a] **P. Seller,**[a] **P.J. Sellin,**[b] **M.C. Veale**[a] **and M.D. Wilson**[a]

[a] *Rutherford Appleton Laboratory, Harwell-Oxford, Oxfordshire, OX11 0QX, U.K.*
[b] *Faculty of Engineering and Physical Sciences, University of Surrey, Guildford, Surrey, GU2 7XH, U.K.*
[c] *National Physical Laboratory, Hampton Road, Teddington, TW11 0LW, U.K.*

E-mail: steven.bell@npl.co.uk

Abstract: Recent improvements in the growth of wide-bandgap semiconductors, such as cadmium zinc telluride (CdZnTe or CZT), has enabled spectroscopic X/γ-ray imaging detectors to be developed. These detectors have applications covering homeland security, industrial analysis, space science and medical imaging. At the Rutherford Appleton Laboratory (RAL) a promising range of spectroscopic, position sensitive, small-pixel Cd(Zn)Te detectors have been developed. The challenge now is to improve the quality of metal contacts on CdZnTe in order to meet the demanding energy and spatial resolution requirements of these applications. The choice of metal deposition method and fabrication process are of fundamental importance. Presented is a comparison of two CdZnTe detectors with contacts formed by sputter and electroless deposition. The detectors were fabricated with a 74×74 array of 200 μm pixels on a 250 μm pitch and bump-bonded to the HEXITEC ASIC. The X/γ-ray emissions from an ^{241}Am source were measured to form energy spectra for comparison. It was found that the detector with contacts formed by electroless deposition produced the best uniformity and energy resolution; the best pixel produced a FWHM of 560 eV at 59.54 keV and 50% of pixels produced a FWHM better than 1.7 keV. This compared with a FWHM of 1.5 keV for the best pixel and 50% of pixels better than 4.4 keV for the detector with sputtered contacts.

Keywords: Gamma detectors (scintillators, CZT, HPG, HgI etc); Hybrid detectors; Materials for solid-state detectors; X-ray detectors

[1] Corresponding author.
[2] The author is now with the National Physical Laboratory however the current work was completed at the Rutherford Appleton Laboratory and the University of Surrey.

https://doi.org/10.1088/1748-0221/12/06/P06015

Contents

1 Introduction **1**

2 Experimental procedure **2**
- 2.1 Detector fabrication 2
- 2.2 Detector hybridization 3
- 2.3 Radiation measurements 3

3 Results and discussion **4**

4 Conclusions and summary **8**

2017 JINST 12 P06015

1 Introduction

Cadmium zinc telluride (CdZnTe or CZT) is a wide-bandgap semiconductor with a high X/γ-ray stopping power, making it well suited as a compact, room temperature radiation detector/imager. This technology is being utilised in the fields of medical imaging, homeland security, industrial analysis and astrophysics [1–5].

Pixellation of the anode contact is required for spectroscopic imaging with Cd(Zn)Te. Smaller pixels provide improved spatial resolution and benefit from the small-pixel effect, as described by the Shockley-Ramo theorem [6, 7]. As the pixel pitch is reduced, the charge cloud created by an X/γ-ray interaction is shared by an increasing numbers of pixels [8]. For X/γ-rays up to 200 keV, a pixel pitch of 250 μm provides good spatial resolution without significant degradation of spectroscopic response due to charge sharing. The deposition of high-quality, uniform, small metal contacts on CdZnTe remains technically challenging and improvements in the crystal preparation, metal deposition, lithography and bonding must be made if CdZnTe is to compete with CdTe and other traditional X/γ-ray sensors.

The Rutherford Appleton Laboratory (RAL), through the HEXITEC collaboration [9], has produced a range of spectroscopic small-pixel CdTe and CdZnTe X/γ-ray imagers and associated ASICs (application specific integrated circuits) [8, 10–12]. This technology have been exploited for medical imaging [13, 14], homeland security [15] and materials science applications [16, 17]. The current work describes the latest advances at RAL in the fabrication of small-pixel CdZnTe detectors. Two methods of gold deposition and pixel fabrication have been investigated; electroless deposition with positive photoresist and sputter deposition with negative photoresist. The choice of fabrication process is partly dictated by the choice of metal deposition method. To enable spectroscopic radiation measurements to be completed, two small-pixel CdZnTe detectors were fabricated and flip-chip bump bonded to the HEXITEC ASIC. The choice of metal deposition method, and a detailed investigation of the metal-semiconductor interface formed by electroless and sputter deposition is discussed in our previous work [18].

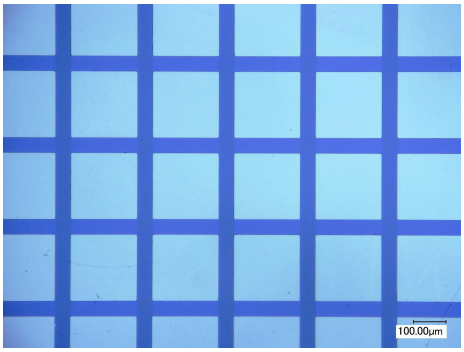

Figure 1. Optical micrograph of a pixel array formed on CdZnTe with positive photoresist and a dark-field mask. The gold was deposited by electroless deposition and the photoresist has been removed.

2 Experimental procedure

2.1 Detector fabrication

The fabrication process involved preparing the crystal, depositing gold contacts and segmenting the anode contact to form a 74×74 array of 200 μm pixels on a 250 μm pitch. A (111) orientated CdZnTe crystal, grown by Redlen Technologies Inc. using the travelling heater method (THM) [19] was diced to form two detectors with dimensions of $20 \times 20 \times 2\,\mathrm{mm}^3$. The crystals were prepared by lapping with 3 μm alumina slurry, followed by a two stage mechanical polish with 0.3 μm and 0.05 μm alumina slurry. It was decided not to chemo-mechanically polish the CdZnTe in order to avoid associated interface non-uniformity and the development of the orange-peel effect [20].

The gold chloride (tetrachloroauric(III) acid) solution contained 30 wt% $HAuCl_4$, 5–10 wt% HCl and 60–65 wt% deionised water giving a ratio of 1:25 for $HAuCl_4$ to H_2O/HCl. To minimise the leakage current associated with contacts deposited at elevated temperatures [20], an ice bath was used to cool the gold chloride solution down to 0 °C. The detectors were cleaned with acetone and isopropanol before being rinsed with deionized water. The crystal edges were protected with photoresist to stop gold formation before being submerged in the gold chloride solution for 3 min. Gold sputtering was performed using an Emitech K575X magnetron sputter coater with a target current of 100 mA for 2 min without heating or cooling the substrate. Following gold deposition the samples were baked at 85 °C for $\sim$ 30 min to improve adhesion.

Photolithography was used to create the pixel array. The detector with electroless contacts was fabricated with a positive photoresist (AZ-9260) and the detector with sputtered contacts was fabricated using a negative photoresist (SU-8-2005). A dark-field mask was used for both. The combination of positive photoresist and dark-field mask (used on the detector with electroless contacts) required the lithography to be completed on the bare CdZnTe substrate before metal deposition. The opaque regions of the mask corresponded to the interpixel channels and the pixel pads were exposed. Exposure of the positive resist allowed it to be removed during development. The interpixel channels remained protected allowing metal to be deposited on the CdZnTe substrate only in the open pad regions. A subsection of the pixel array produced by this method is shown in figure 1. The pixel definition was found to be very good, with a consistent interpixel gap of $\sim$ 47 μm, close to the target of 50 μm. The interpixel resistance was measured to be $1.7 \pm 0.5 \times 10^{11}\ \Omega$.

2017 JINST 12 P06015

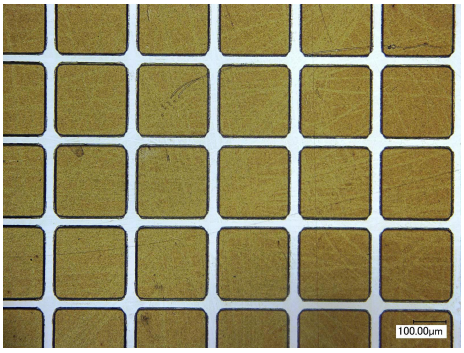

Figure 2. Optical micrograph of a pixel array formed on CdZnTe with negative photoresist and a dark-field mask. The gold was deposited by sputter deposition and the interpixel gold has been etched away with 5% bromine-in-methanol.

Stripping or lifting off the photoresist is required if metal coats the resist in the interpixel channels. This does not occur during electroless deposition as the chloride solution only reacts with the exposed CdZnTe. However, this does occur during sputter deposition. The conformal nature of the gold coating makes lift off of the photoresist very difficult meaning that this process cannot be considered compatible with sputter deposition. This is the reason for the use of negative photoresist with the sputter contacted detector.

The combination of negative photoresist and dark-field mask required planar metal contacts to be deposited on the bare CdZnTe substrate before lithography. The opaque regions of the mask corresponded to the interpixel channels. This allowed the pixel pad regions to be exposed and cross-linked and the interpixel channels were subsequently removed during development. The pixel pads were protected allowing the metal in the open interpixel channels to be etched away. This was achieved with a 3 min treatment with 5% bromine-in-methanol. The definition of the individual pixels was good (see figure 2), albeit slightly over sized, with the interpixel gap reduced to $\sim 25\ \mu$m in the centre of the detector and $\sim 35\ \mu$m at the edges of the detector. The interpixel resistance was measured to be $\sim 10^9\ \Omega$; two orders of magnitude lower than the detector with electroless gold contacts that did not require etching to remove interpixel gold.

2.2 Detector hybridization

Hybrid detector assemblies were formed by bonding the fabricated pixel detectors to the HEXITEC ASIC. This procedure began by thermosonically bonding gold studs to the ASIC pixels using a Palomar P8000 wafer bonder. Next, a conductive silver-loaded epoxy was printed across the pixel array of the fabricated detector using a custom-built stencil printer. Finally, the studded ASIC and detector were brought into close alignment and bonded at low pressure (~0.8 mN/bump) and temperature (30 °C) using a SET FC150 flip-chip bonder. The hybridized assembly was cured at 45 °C for an extended period to ensure the epoxy had set without introducing thermal stress into the bonds. The bonding process is described in greater detail in our previous work [21].

2.3 Radiation measurements

The fabricated and assembled detectors were exposed to a 185 MBq ^{241}Am radiation point source positioned 10 cm directly in front of the sensor. The peak centroid and intensity of the primary

2017 JINST 12 P06015

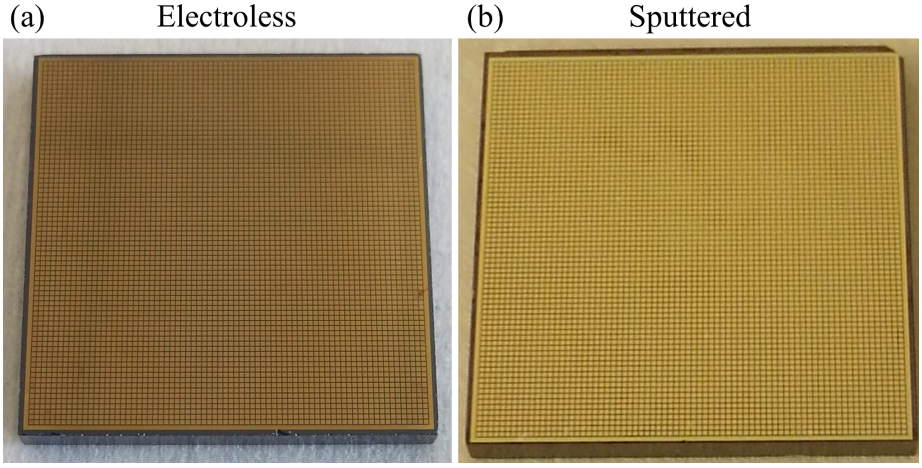

Figure 3. Photographs of small-pixel CdZnTe detectors with gold contacts formed by (a) electroless and (b) sputter deposition before bonding.

^{241}Am gamma emission at 59.54 keV was recorded for all pixels to determine the uniformity of response across the pixel array. The full width at half maximum (FWHM) of the 59.54 keV photopeak was measured to determine the energy resolution of each pixel and again assess the uniformity of response. The data was processed with custom Matlab scripts written at RAL. The measured spectra were corrected for charge sharing, which involved removing events where one or more of the four nearest neighbours recorded an event in the same frame [22].

The operating bias and temperature of each detector was chosen to optimize performance; high bias for improved charge collection and low temperature to reduce leakage current. Eventually dielectric breakdown, elevated leakage currents or bias-induced polarization limited the bias that could be applied. This occurred at a lower bias for the sputtered contacts because of effects other than differing pixel size (e.g. different barrier heights, interface structure etc.) The efficiency of the Peltier cooler limited how low the temperature could be reduced. The Peltier bonded to the sputtered detector hybrid module was less effective at cooling the ASIC compared with the one mounted on the electroless detector module. The final operating conditions were; −750 V and 4.5 °C for the detector with electroless contacts, and −700 V and 11°C for the detector with sputtered contacts. In our experience, the small differences in bias and operating temperature would not be sufficient to produce significantly different spectral response of the two detectors.

3 Results and discussion

Two small-pixel CdZnTe detectors were fabricated and flip-chip bump bonded to the HEXITEC ASIC for X/γ-ray testing. One detector had electroless gold contacts and the other, sputtered gold contacts. The (111)A Cd-face of the crystal was patterned with a 250 μm pitch 74 × 74 pixel array and a guard band structure. A planar gold contact was deposited on the (111)B Te-face and radiation measurements of a ^{241}Am source were completed. The two fabricated detectors are shown in figure 3 before being bonded to the HEXITEC ASIC.

2017 JINST 12 P06015

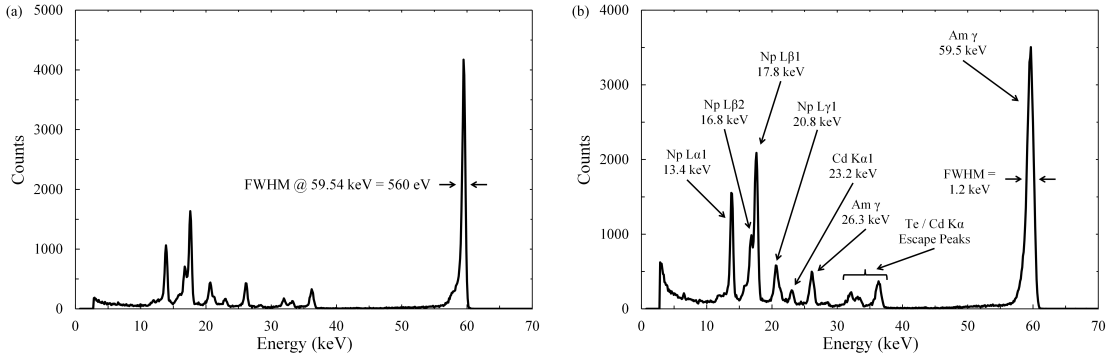

Figure 4. Examples of (a) the best and (b) the modal single pixel spectra measured across the 74×74 pixels of the CdZnTe HEXITEC detector with electroless gold contacts exposed to a ^{241}Am point source. The resolvable X/γ lines have been identified in (b).

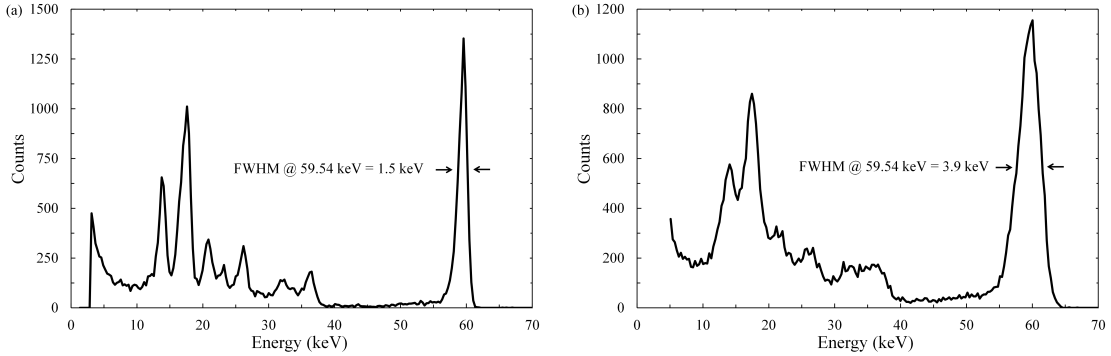

Figure 5. Examples of (a) the best and (b) the modal single pixel spectra measured across the 74×74 pixels of the CdZnTe HEXITEC detector with sputtered gold contacts exposed to a ^{241}Am point source.

Example single pixel spectra demonstrating the best and modal FWHM energy resolutions measured at the 59.54 keV photopeak for the detectors with electroless and sputtered gold contacts are presented in figure 4 and figure 5 respectively.

Histograms of the FWHM values measured across all pixels of both detectors are shown in figure 6. For the detector with electroless contacts, the best performing pixel produced a FWHM resolution of 560 eV and the modal FWHM value was 1.2 keV with a standard deviation of 0.4 keV. 50% of pixels produced a FWHM better than 1.7 keV. To the authors' knowledge, to date the best reported FWHM at 59.54 keV for CdTe or CdZnTe is 600 eV (XR-100T-CdTe detector from AMPTEK [23]). The AMPTEK system included a rise-time discriminator to correct for hole trapping. The HEXITEC system does not have a rise-time discriminator and instead utilises the small-pixel effect. The spectra measured with the HEXITEC CdZnTe detectors displayed a small degree of low energy tailing however this was likely related to incomplete collection of electrons due to trapping and electric field effects as much as the incomplete collection of holes. The shoulder extending for $\sim$ 2 keV below the 59.54 keV photopeak in figure 4(a) was a result of the charge sharing discrimination algorithm missing shared events where a fraction of charge less than the low energy threshold of the pixel ($\sim$ 2 keV) was shared with a neighbour [22].

2017 JINST 12 P06015

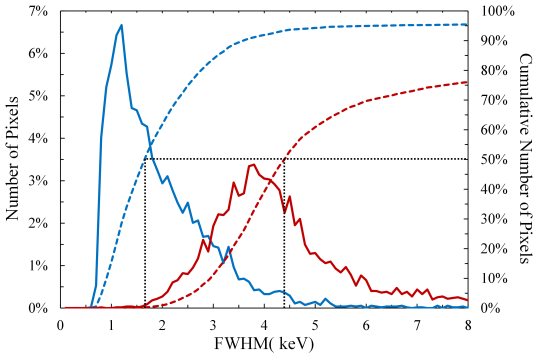

Figure 6. The distribution of FWHM values of the 59.54 keV ^{241}Am γ-ray photopeak for all 74 × 74 pixels of CdZnTe HEXITEC detectors with electroless (blue) and sputtered (red) gold contacts. The right hand axis shows the cumulative number of pixels as a function of FWHM (broken lines). The dotted lines mark the FWHM values attained by 50% of pixels.

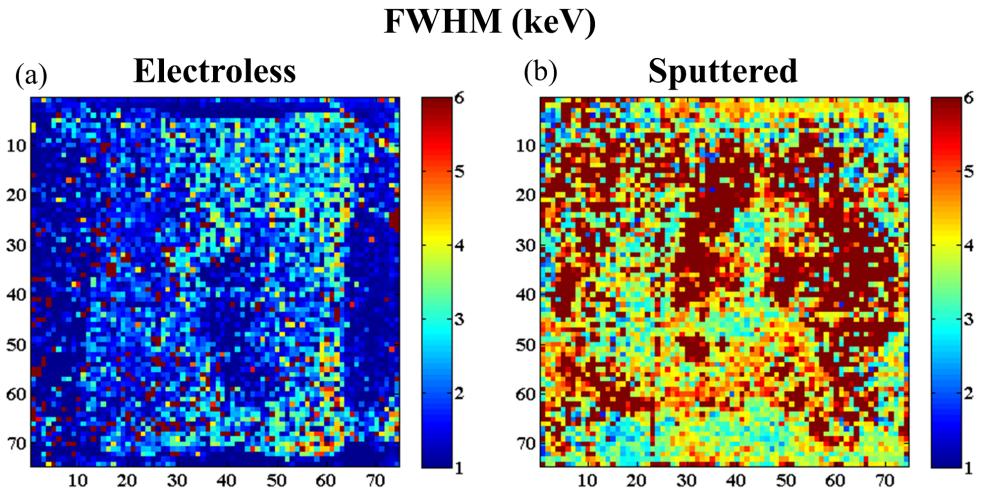

Figure 7. The FWHM of the 59.54 keV γ-ray photopeak for all 74 × 74 pixels of CdZnTe detectors with (a) electroless and (b) sputtered contacts. Dead pixels and pixels with a FWHM > 6 keV are shown as dark red.

For the detector with sputtered contacts, the best performing pixel produced a FWHM resolution of 1.5 keV and the modal FWHM value was 3.9 keV with a standard deviation of 0.9 keV. 50% of pixels produced a FWHM better than 4.4 keV. The photopeaks in the spectrum with 3.9 keV FWHM showed signs of tailing towards lower energies. This may have been due to crystal defects and impurities trapping charge, possibly related to the use of an insufficient bias to achieve full charge collection. The field strength of 3,500 V.cm^{-1} used in the current work is typically sufficient for complete charge collection in CdTe/CdZnTe detectors [24]. It was not feasible to increase the bias due to the exponential increase in leakage current and reduction in leakage current stability observed at higher bias.

The FWHM, peak position and peak counts of the 59.54 keV gamma emission were calculated for all 74×74 pixels using a MATLAB script and the results are presented in figures 7–9 respectively.

The detector with sputtered contacts was found to have 790 non-spectroscopic pixels. This represented 14% of the total 5,476 pixels. This compared with 193 (4%) non-spectroscopic pixels for the detector with electroless contacts. Pixels were considered to be non-spectroscopic if they were

2017 JINST 12 P06015

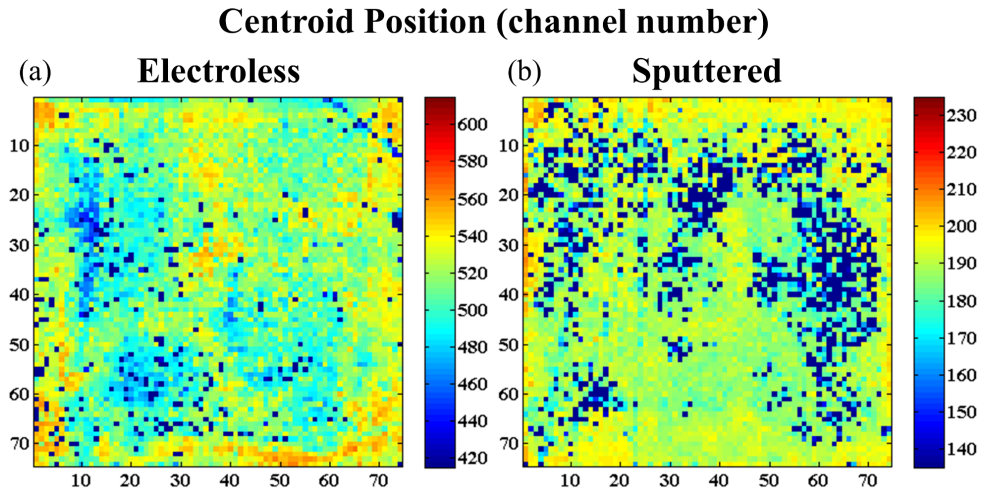

Figure 8. The centroid channel position of the 59.54 keV γ-ray photopeak for all 74×74 pixels of CdZnTe detectors with (a) electroless and (b) sputtered gold contacts. The scale of each plot has been centred on the average channel position and extends proportionately over the same range; 515 ± 100 and 185 ± 50 channels respectively. Dead or severely low gain pixels are shown as dark blue.

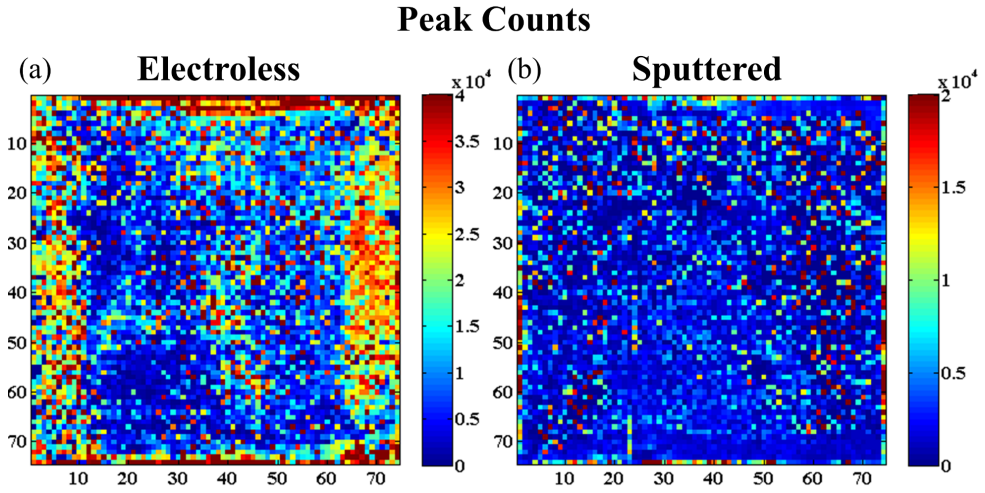

Figure 9. The number of counts in the 59.54 keV γ-ray photopeak for all 74×74 pixels of CdZnTe detectors with (a) electroless and (b) sputtered gold contacts. The acquisition time for the detector with electroless contacts was 2 hr, twice as long as that for the detector with sputtered contacts. The scale of each plot has been adjusted accordingly.

dominated by electronic noise, had extremely low counts or low gain, or produced no discernible spectrum. There are several possible reasons why the spectral response of a pixel may be poor, including inclusions and crystal defects [25], failed bonds, electric field effects [25–27] and edge effects [28, 29]. For imaging applications, spectra from such pixels would likely be disregarded and the image interpolated from neighbouring pixels [30]. If a pixel produced a significantly degraded spectrum due to one or more of the above mentioned phenomena, then the spectrum was disregarded from further analysis. These pixels appeared as dark red pixels in the FWHM distribution maps of

2017 JINST 12 P06015

figure 7 and as dark blue pixels in the centroid position maps of figure 8.

It was not possible to determine if either of the contacting methods, sputter or electroless deposition, was likely to produce more or less non-spectroscopic pixels as the two detectors investigated were pixellated following different lithographic methods. The pixellation of the detector with sputtered contacts involved etching away the gold from the interpixel channel with bromine-in-methanol. The bromine etchant produced a trench several μm into the CdZnTe bulk. Interpixel resistance measurements on detectors fabricated under similar conditions indicated that etched interpixel channels had a lower resistance than non-etched bare CdZnTe interpixel channels ($\sim 10^9\,\Omega$ compared with $\sim 10^{11}\,\Omega$ respectively) [31]. Even when the etched interpixel channel was passivated the resistance was still over an order of magnitude lower than the non-etched channel. A low interpixel resistance can lead to charge drifting towards the crystal surface between pixels and not being funnelled towards and collected by the pixel contact [28]. It was not possible to determine the uniformity of the etch across the pixel array. If a variation in defect density and resistance along the interpixel trenches existed it is possible that localised perturbations in the electric field would have detrimentally affected the spectroscopic response of certain pixels. It was identified that undercutting and subsequent peeling of the gold pixel contact was also possible during interpixel etching. A further issue identified with the negative photoresist/dark-field mask lithographic method was the possibility that residual photoresist remained on the pixel after the photoresist lift off. This may have increased the capacitance of the pixel and reduced the pixel gain such that the 59.54 keV photopeak was no longer in the region of interest specified in the MATLAB calibration algorithm. Such low gain pixels may have presented good energy resolution but would have been rejected as "non-spectroscopic". As the spectrum shape was known (^{241}Am gamma spectrum), it would have been possible to amend the calibration algorithm to correct the low gain pixels. It was decided not to do this as eventually these detectors will be used to measure unknown spectra. A significant variation from pixel-to-pixel could produce unpredictable behavior with the fitting algorithm, producing erroneous results. Also, the reduced gain has the effect of squashing the spectrum into less channels, which reduces the potential energy resolution.

The detector with electroless contacts did not require interpixel etching. As such the interpixel channels were likely to have better uniformity and higher resistance. The detector with electroless contacts also did not require photoresist to be deposited on the gold pixel contacts and so residue was less likely to be present. It is for these reasons that the detector with sputtered contacts was found to have significantly more non-spectroscopic pixels compared with the detector with electroless contacts. Non-uniformity of the crystal may also be responsible for spatial variation and the degraded spectral response of some pixels. It is however unlikely that crystal non-uniformity is responsible for the observed differences as both detectors were diced from the same crystal.

4 Conclusions and summary

The fabrication of small-pixel CdZnTe detectors with gold contacts deposited by electroless and sputter deposition has been investigated. The spectroscopic performance was determined by bonding the detectors to the HEXITEC ASIC and exposing to a ^{241}Am X/γ-ray source.

The detector with contacts formed by electroless deposition was measured to produce a superior spectral response compared with the detector with sputtered contacts. The best performing pixel

2017 JINST 12 P06015

produced a FWHM energy resolution of 560 eV at 59.54 keV, comparable to the best reported in the literature. This compared with 1.5 keV for the detector with sputtered contacts. The uniformity and pixel yield was also higher for the detector with electroless contacts. The interpixel etching, which was required to pixellate the detector with sputtered contacts, was the cause of the reduced yield of spectroscopic pixels in this detector. For the detector with electroless contacts, it was not necessary to etch the interpixel region and as a result the pixel yield was better. It was not possible to perform the same procedure (positive photoresist, dark-field mask) with the sputtered detector due to the conformal nature of the sputter coating. Instead, a negative photoresist and dark-field mask procedure was used and this proved to be less reliable and resulted in different pixel sizes. This in its self is an important technical outcome of the work.

Developing a deposition method and compatible pixellation process is vital if CdZnTe X/γ-ray imagers are to replace traditional technologies. The presented results represent an important step towards achieving uniform, high resolution small-pixel CdZnTe detectors.

Acknowledgments

This research was funded by the EPSRC (grant EP/G037388/1) via the MiNMaT Industrial Doctorial Centre of the University of Surrey in collaboration with the Centre for Instrumentation at the Rutherford Appleton Laboratory (Science and Technology Facilities Council).

References

[1] T.E. Schlesinger et al., *Cadmium Zinc Telluride and its use as a nuclear radiation detector material*, *Mater. Sci. Engineer. Rept.* **32** (2001) 103.

[2] A. Owens and A. Peacock, *Compound semiconductor radiation detectors*, *Nucl. Instrum. Meth.* **A 531** (2004) 18.

[3] C. Szeles et al., *CdZnTe semiconductor detectors for spectroscopic X-ray imaging*, *IEEE Trans. Nucl. Sci.* **55** (2008) 572.

[4] S. del Sordo et al., *Progress in the Development of CdTe and CdZTe Semiconductor Radiation Detectors for Astrophysical and Medical Applications*, *Sensors* **9** (2009) 3491.

[5] S.V. Vadawale et al., *Hard X-ray continuum from lunar surface: results from High Energy X-ray Spectrometer (HEX) onboard Chandrayaan-1*, *Adv. Space Res.* **54** (2014) 2041.

[6] W. Shockley, *Currents to conductors induced by a moving charge*, *J. Appl. Phys.* **9** (1938) 635.

[7] S. Ramo, *Currents induced by electron motion*, *Proc. IRE* **27** (1939) 584.

[8] M.C. Veale et al., *An ASIC for the study of charge sharing effects in small-pixel CdZnTe X-ray detectors*, *IEEE Trans. Nucl. Sci.* **58** (2011) 2357.

[9] M.C. Veale, *HEXITEC, Homepage of Rutherford Appleton Laboratory*, http://en.wikipedia.org/wiki/HEXITEC (2017).

[10] L.L. Jones et al., *HEXITEC ASIC — A pixellated readout chip for CZT detectors*, *Nucl. Instrum Meth.* **A 604** (2009) 34.

[11] P. Seller et al., *Pixellated Cd(Zn)Te high-energy X-ray instrument*, 2011 *JINST* **6** C12009.

2017 JINST 12 P06015

[12] M.D. Wilson et al., *A 10 cm ×10 cm CdTe spectroscopic imaging detector based on the HEXITEC ASIC*, 2015 *JINST* **10** P10011.

[13] S. Pani et al., *K-edge subtraction imaging using a pixellated energy-resolving detector*, *Proc. SPIE* (2011) 7961.

[14] J.W. Scuffham et al., *A CdTe detector for hyperspectral SPECT imaging*, 2012 *JINST* **7** P08027.

[15] D. O'Flynn, *Identification of simulants for explosives using pixellated X-ray diffraction*, *Crime Sci.* **2** (2013) 4.

[16] E. Liotti et al., *Mapping of multi-elements during melting and solidification using synchrotron X-rays and pixel-based spectroscopy*, *Nature Sci. Rept.* **5** (2015) 15988.

[17] C. Egan et al., *3D chemical imaging in the laboratory by hyperspectral X-ray computed tomography*, *Nature Sci. Rept.* **5** (2015) 15979.

[18] S.J. Bell et al., *Comparison of the surfaces and interfaces formed for sputter and electroless deposited gold contacts on CdZnTe*, submitted to *Appl. Surf. Sci.* (2017).

[19] M. Amman et al., *Evaluation of THM-grown CdZnTe material for large-volume gamma-ray detector applications*, *IEEE Tran. Nucl. Sci.* **56** (2009) 795.

[20] S.J. Bell et al., *Characterization of the metal-semiconductor interface of gold contacts on CdZnTe formed by electroless deposition*, *J. Phys.* **D 48** (2015) 275304.

[21] A. Schneider et al., *Interconnect and bonding techniques for pixelated X-ray and gamma-ray detectors*, 2014 *JINST* **10** C02010.

[22] M.C. Veale et al., *Measurements of charge sharing in small-pixel CdTe detectors*, *Nucl. Instrum. Meth.* **A 767** (2014) 218.

[23] *AMPTEK, XR-100T-CdTe*, http://www.amptek.com/wp-content/uploads/2014/04/XR-100T-CdTe-X-ray-and-Gamma-Ray-Detector-Specifications.pdf
(2017).

[24] M.C. Veale, *Charge transport and low temperature phenomena in single crystal CdZnTe*, University of Surrey, Guildford, U.K. (2009).

[25] A.E. Bolotnikov et al., *Characterization and evaluation of extended defects in CZT crystals and gamma-ray Detectors*, *J. Cryst. Growth* **379** (2013) 46.

[26] A.E. Bolotnikov et al., *Charge loss between contacts of CdZnTe pixel detectors*, *Nucl. Instrum. Meth.* **A 432** (1999) 326.

[27] M.C. Veale et al., *Synchrotron characterisation of non-uniformities in a small-pixel Cadmium Zinc Telluride imaging detector*, *Nucl. Instrum. Meth.* **A 729** (2013) 265.

[28] A.E. Bolotnikov et al., *Internal electric-field-lines distribution in CdZnTe detectors measured using X-ray mapping*, *IEEE Trans. Nucl. Sci.* **56** (2009) 791.

[29] D.D. Duarte et al., *Edge effects in a small-pixel CdTe for X-ray imaging*, 2013 *JINST* **8** P10018.

[30] J.T. Bushberg et al., *The essential physics of medical imaging*, second edition, Lippincott Williams & Wilkins, Philadelphia U.S.A. (2002).

[31] S.J. Bell, *Fabrication and characterisation of gold contacts on CdZnTe radiation detectors*, Eng.D. Thesis, University of Surrey, Guildford, U.K. (2015).

2017 JINST 12 P06015